Heliyon 7 (2021) e06064

Contents lists available at ScienceDirect

Heliyon

journal homepage: www.cell.com/heliyon

Research article

Crystal growth inhibition of gypsum under normal conditions and high supersaturations by a copolymer of phosphino-polycarboxylic acid

Keyvan Malaie, Omid Shojaei *, Saeed Iranpour, Zohreh Taherkhani

Chemical Process Design Research Group, ACECR, Faculty of Engineering, University of Tehran, Tehran, Iran

ARTICLE INFO

Keywords:
Gypsum
Phosphino-polycarboxylic acid
Scale
Inhibitor

ABSTRACT

Scale formation is a bottleneck of most industrial and domestic water equipment, in particular, of oilfield water systems. Therefore, high-performance and environmentally-benign chemical scale inhibitors are highly needed. Phosphino-polycarboxylic acid (PPCA) is a low-in-phosphorous scale inhibitor with high inhibition efficiency, but its synthesis and performance analyses have been rarely disclosed. In this work for the first time, a PPCA copolymer is synthesized by a simple method based on free radical polymerization of acrylic acid and phosphinic acid monomers and directly employed for gypsum scale inhibition. The formation of PPCA was verified by FTIR and ^{31}PNMR spectroscopies, and then its inhibition performance was evaluated by the complexometric determination of the Ca^{2+} concentration. The PPCA (2.5 ppm) showed 100% inhibition efficiency at a saturation index of 0.31 at the room temperature and without pH regulation after 24 h with practically no detectable gypsum crystallites even after two months, while the commercial ATMP showed a low inhibition efficiency of 30%. The Field Emission Scanning Microscopy (FESEM) images of the PPCA-inhibited and uninhibited samples revealed that the typical gypsum microfibers are distorted and reduced in size significantly in the inhibited sample. At a still higher saturation index of 1.47 (saturation ratio of 10), the inhibition efficiency of PPCA reduced to 16% and 24% for two dosages of 2.5 and 10 ppm which was attributed to the higher ion activity coefficients at the extremely high ionic strength, and hence, a much higher thermodynamic driving force. The rate constants for these two high supersaturation conditions and low PPCA dosages were also calculated and discussed.

1. Introduction

Scale deposition or the precipitation of inorganic salts is a serious problem in industrial and domestic waters. It could lead to the blockage of pipelines and equipment, energy leak, or even increased corrosion [1, 2]; therefore, it incurs extra budgets on companies to prevent or remove the scale in order to maintain the efficient flow of water systems. In oil production, scale formation can occur during different processes including water injection, oil extraction, transportation, and thermal (or chemical) treatments [3]. Scale deposition is also a bottleneck of current reverse-osmosis water purification filters [4], heat exchangers [5, 6], boilers [7], and other equipment.

Scale deposition is the direct consequence of the thermodynamic conditions of the system; in other words, when the amount of a cation and anion raise above their saturation level due to various causes, they ultimately deposit on the equipment surfaces. Sparingly soluble salts such as calcium carbonate, calcium sulfate, barium sulfate, strontium sulfate, and other sediments constitute the common scales. Among them, though calcium sulfate (i.e., anhydrite ($CaSO_4$) or gypsum ($CaSO_4.2H_2O$)) has the highest solubility, it is widely occurring due to the high crustal abundance of calcium and sulfate ions [8, 9] as well as its pH-independent low solubility that make gypsum scale inhibition highly challenging [13].

Currently, the problem of scale formation is generally tackled by the traditional physical methods or a combination of physical and chemical methods. For example, the water purification filters or oilfield water equipment are regularly dismantled to physically remove the scale. Other methods include acid treatment, thermal or magnetic radiation, as well as the addition of chelating agents such as ethylenediamine-tetraacetic acid (EDTA). However, none of these methods have acceptable efficiency at a reasonable cost. For instance, EDTA is a very good chelating agent for alkaline earth metal cations, and an equivalent amount would practically chelate all the cations and prevent scaling, but for industrial processes it is a costly method; it also requires specific conditions such as regulated pH and water hardness, and also it may increase corrosion rate [10, 11].

* Corresponding author.
E-mail address: Omidshojaei@ut.ac.ir (O. Shojaei).

https://doi.org/10.1016/j.heliyon.2021.e06064
Received 7 September 2020; Received in revised form 22 October 2020; Accepted 19 January 2021

The most efficient and economic method of scale prevention is treating the water with chemical scale inhibitors such as (poly) phosphonates, polyacrylamide, polymaleic acid, and polycarboxylates [10]. They are also called threshold scale inhibition agents, because they are only required at micro-molar amounts far below the stoichiometric level to exhibit their highest effect. Generally, their effect is correlated with an increase in the crystal/solution interfacial tension. For instance, the HDTMP and HEDP inhibitors increase the interfacial tension and prolong the nucleation induction period for calcium sulfate [11]. Mechanistically, the inhibition is assumed to occur either at nucleation stage based on re-dissolving the early crystal nuclei by the endothermic adsorption (or interaction) of the inhibitor, or at growth stage through adsorption of inhibitor on the active growth sites; However, in reality scale inhibitors may work based on both mechanisms. The effectiveness of the polymeric inhibitors depends on their functional groups, molar mass, and charge density, in addition to the experimental conditions such as temperature, pH, ionic strength, degree of supersaturation, and cation/anion molar ratio [12, 13].

(Poly) phosphonates have a good inhibition efficiency and are widely studied for gypsum scale inhibition. However, they are susceptible to hydrolysis and may increase the orthophosphates and other phosphorous compounds that react with calcium ions to produce other insoluble salts. Besides, the release of these phosphorous compounds can cause aquatic eutrophication that distorts the environment. More environmentally-benign and yet efficient chemical inhibitors are based on the co-polymers of acrylate such as acrylic acid-maleic acid or acrylamide-maleic acid [8, 14]. A well-known inhibitor, phosphino-polycarboxylic acid (PPCA, Scheme 1) is based on acrylate and phosphonate monomers and combines the advantages of both units. Besides, phosphonates are usually growth inhibitors and polyacrylates are nucleation inhibitors, and therefore, their combination can create a synergistic effect.

Nevertheless, the PPCA has not gained a wide application for the inhibition of gypsum and other scales since their introduction three decades ago, which could be attributed to the lack of enough information on their preparation methods and performance analysis that is limited to several communications [15, 16, 17, 18]. The synthesis procedures for PPCA-based inhibitors are stored exclusively in several patents [19] and companies' repositories. Furthermore, the previous studies have focused on the effect of temperature/pressure [20], squeeze treatment modes [15], polymer molecular weight [16, 21], chemical modification [22, 23], as well as its chemical analogues (phosphono/phosphoryl carboxylic acid polymers [24, 25]), while, to the best of our knowledge, there is no report on the chemical synthesis and performance analysis of the PPCA copolymer under normal environmental conditions and high supersaturations.

This study was conducted to evaluate the scale inhibition efficiency of a PPCA copolymer, synthesized by a free radical polymerization, under normal conditions (25 °C, 1 atm, and initial pH of ~7) but at high saturation indexes of SI = 0.31 and SI = 1.47. The results for gypsum inhibition by the as-synthesized PPCA indicate that although PPCA perform excellent with an inhibition efficiency of 100% compared to 30% for commercial ATMP in 24 h, gypsum inhibition becomes highly challenging under the extreme supersaturation condition of SI = 1.45 even with PPCA. This decrease of efficiency was attributed to the curving-up of the ionic activity coefficient-ionic strength that creates a high thermodynamic driving force for gypsum formation.

2. Experimental

2.1. Reagents

Acrylic acid (99%), hypophosphorous acid (also called phosphinic acid) solution (50%), benzoyl peroxide (75%) were obtained from Sigma-Aldrich and used as precursors for the synthesis of PPCA. Calcium chloride ($CaCl_2.2H_2O$, 99%), sodium sulfate (Na_2SO_4, %99), ethylenediamine-tetraacetic acid (EDTA), murexide ($C_8H_8N_6O_6$), and the reference inhibitor Amino Trimethylene Phosphinic Acid (ATMP, 50 wt. % in H_2O) were also obtained from Sigma-Aldrich. Sodium chloride (NaCl, >98%) was purchased from the Tehran Bazar and used for maintaining the ionic strength of the solutions. Filter papers (Whatman paper 42, pore size ≤ 2.5 μm) were obtained from Whatman Company.

2.2. Synthesis of PPCA copolymer

The PPCA inhibitor was synthesized by a simple chemical method based on the free radical polymerization of monomers. For this purpose, the acrylic acid and phosphinic acid monomers with a molar ratio of 8:1 were used. This molar ratio was selected after repeating the synthesis experiments in order to obtain a complete reaction between the monomers. In a typical process, first 58.22 g acrylic acid and 13.2 g phosphinic acid were added to 50 mL of deionized water under stirring in a three-neck round bottom flask connected to a condenser. Next, 0.25 g benzoyl peroxide as initiator was added slowly, and then, the temperature was slowly raised to 96 °C and kept at this temperature for 5 h. Finally, the flask was slowly cooled to room temperature, and a clear and relatively viscous solution was obtained. The as-obtained PPCA solution was directly used for the next analyses.

2.3. Preparation of supersaturated samples

For the preparation of supersaturated samples, first the reference brine solutions of calcium chloride and sodium sulfate were prepared separately each containing excessive amounts of sodium chloride added as supporting electrolyte. Then, they were filtered to remove possible undissolved particles. 50 mL of calcium-containing brines were transferred to different bottles which had been cleansed carefully. Then, specified amounts of diluted inhibitor samples were spiked in each bottle except the bottle denoted as the blank (or control). Finally, equal volumes of sulfate-containing brines were added into each bottle, and after sealing and shaking, they were immediately transferred into a water bath kept at a temperature of 25 (±0.5) °C. No pH-buffering compounds were used in order to avoid their interference with the performance of the inhibitors.

2.4. Characterization methods and instruments

All the kinetic studies and performance analysis of the scale inhibition were carried out by following the concentration of calcium ion in the solution using conventional complexometric titration with EDTA in the presence of murexide as indicator. For the measurements, the supersaturation solutions were sampled at different time intervals, and immediately filtered and titrated.

The gypsum phase structure was analyzed by X-ray diffraction (XRD) on a Philips PW-1730 X-ray diffractometer using Cu Kα radiation (λ = 1.5405 Å). Surface morphology of the gypsum was characterized by field emission scanning electron microscopy (FESEM) on a Zeiss SIGMA VP. The PPCA was characterized by Fourier Transform Infrared (FTIR) spectrometer (Tensor 27, Bruker Co.) and phosphorus-31 nuclear magnetic resonance (D_2O-PNMR, Bruker Co.).

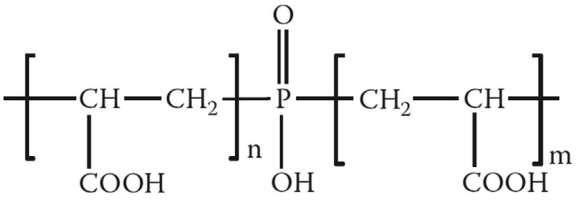

Scheme 1. Phosphino-polycarboxylic acid (PPCA).

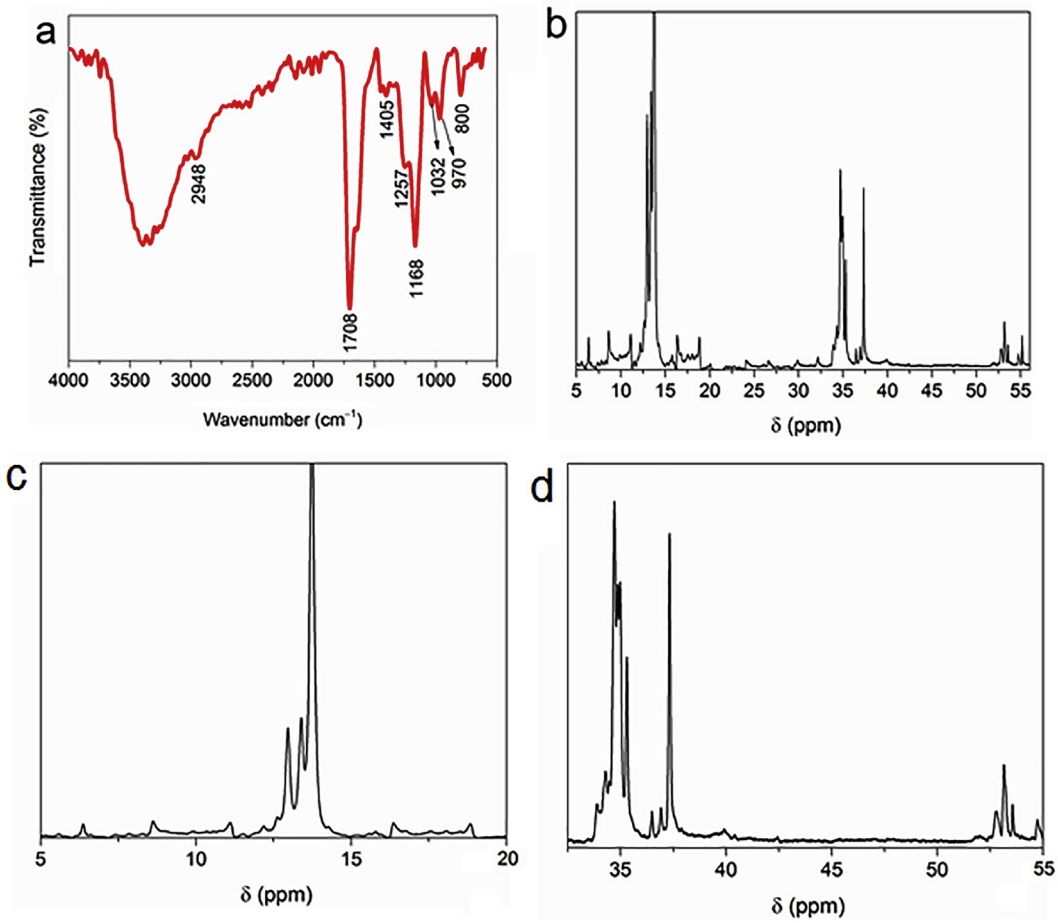

Figure 1. Spectroscopic characterization of the as-synthesized PPCA. (a) IR and (b) ^{31}P NMR spectra. (c) and (d) are the magnified views of the same ^{31}P NMR spectrum.

2.5. Inhibition performance analysis

The following relationships were used for calculating the saturation indexes (SI, Eq. (1)) and the Gibbs free energies of gypsum crystallization (ΔG, Eq. (2)) [11]:

$$SI = \text{Log}\ (\frac{IAP}{K_{sp}}) \quad (1)$$

$$\Delta G = -\frac{RT}{\nu}\ln(\frac{IAP}{K_{sp}}) \quad (2)$$

In the above relationships, IAP is ion activity product, ν is number of ions per formula unit of the electrolyte, and the other symbols have their usual meanings.

The rate constants (k) of gypsum crystallization when the Ca^{2+}/SO_4^{3-} is 1 can be calculated through the integrated form of the following relationship (Eqs. (3) and (4)) that is based on the equimolar reactants

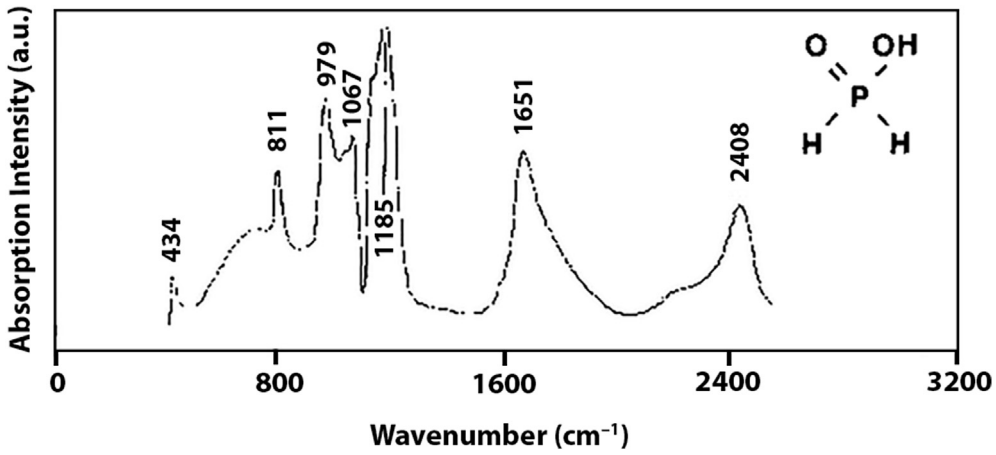

Figure 2. IR absorption spectrum of phosphinic acid in water. (Adapted from ref. [27] Copyright 2020, with permission from Elsevier).

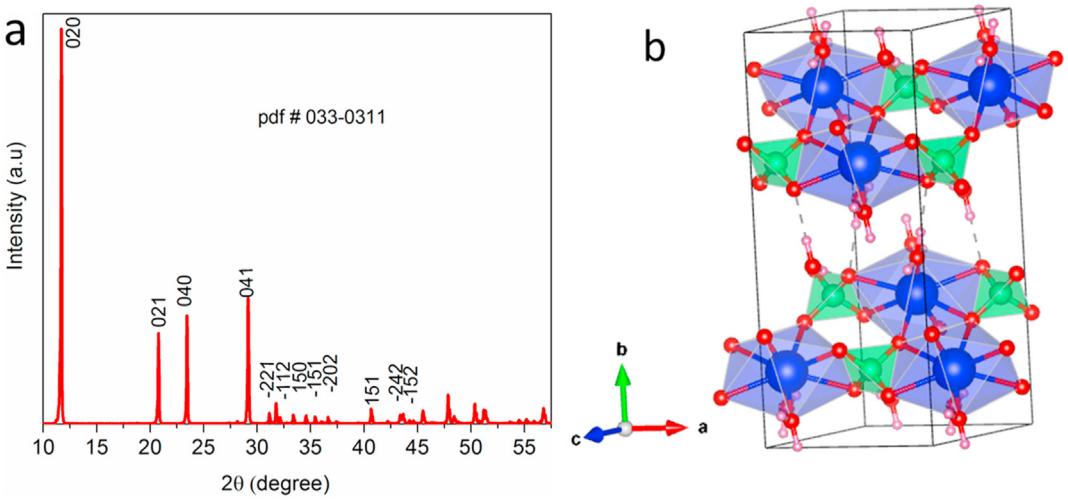

Figure 3. (a) XRD of gypsum precipitated from the uninhibited blank sample and (b) a schematic illustration of its crystal structure.

approaching equilibrium by a second order reaction, proposed first by Nancolas et al. for gypsum crystallization [26]:

$$\text{Differential form: } -\frac{dC}{dt} = k(C - C_{eq})^2 \quad (3)$$

$$\text{Integrated form: } \frac{1}{(C - C_{eq})} = kt + \text{Const} \quad (4)$$

where C and C_{eq} are the total calcium concentration and solubility at reaction temperature.

The inhibition efficiency (IE, eq. 5) of the inhibitors are calculated via the following relationship:

$$\%IE = \frac{C_{inh} - C_{un}}{C^0 - C_{un}} \times 100 \quad (5)$$

Here, the C_{inh}, C_{un}, and C^0 are the total concentrations of calcium in the inhibited sample, uninhibited sample, and in the sample before crystallization (i.e., t = 0).

All inhibition efficiencies were calculated 24 h after creating the supersaturation condition and adding the inhibitor simultaneously. All calcium and sulfate brines were filtered with the Whatman paper to ensure best condition for homogeneous nucleation. Likewise, all supersaturated samples were filtered immediately before registering calcium concentration to minimize error. Besides, all the induction times are reported in an approximate way by visual detection of first crystallites, and therefore, are not comparable with induction times from the literature that are usually measured by some instrument for critical nuclei formation. Furthermore, all tests were carried out two times at least, and the results were expressed as the average of these two values. The error was below 7%, typically.

3. Results

3.1. Characterization of the PPCA

Figure 1a shows the IR spectrum of the as-synthesized PPCA, and Figure 2 shows the IR spectrum of the phosphinic acid reported in the literature for comparison. The IR bands that belong to (poly)carboxylic acid are always easily detectable due to their very intense appearance at 2400–3400, 1700–1725 cm^{-1} and ~1260 cm^{-1}.

Here, the strong bands at 1708 cm^{-1} and 1256 cm^{-1} are due to C=O and C—O stretching vibrations in the polycarboxylic acid, respectively. The broad peak that covers the area from 2300 to 3700 cm^{-1} belongs to the O—H stretching vibration from three different origins: the hydroxyls in the polycarboxylic acid and the phosphinic acid, as well as the water content of the sample. The bands at 1405, 1168, and 970 cm^{-1} are due to, P–CH_2, P=O, P–OH stretching vibrations [27]. Furthermore, the IR spectrum of the phosphinic acid monomer (Figure 2) shows a peak at ~2408 cm^{-1} due to the PH_2 stretching vibration which is absent in the IR spectrum of the PPCA product, confirming successful formation of the

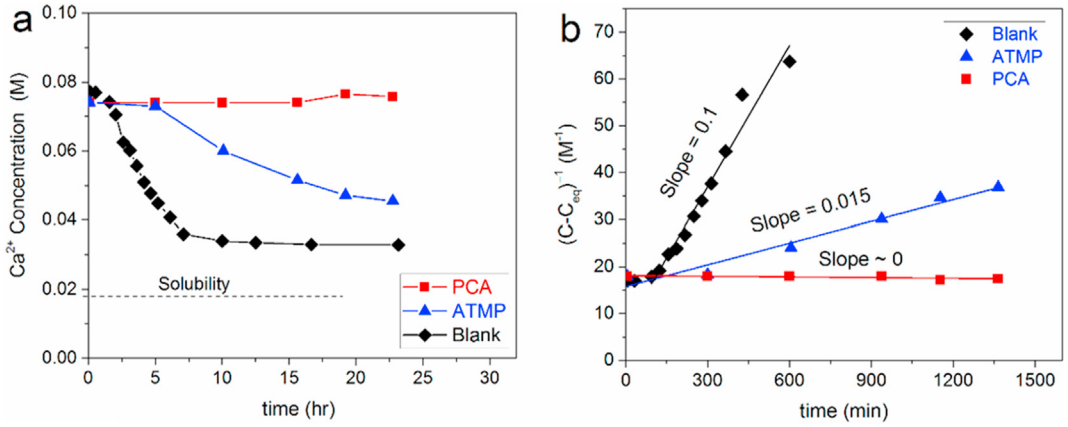

Figure 4. Calcium ion concentration at different times (a) and the corresponding rate constants (b) for supersaturated samples containing 2.5 ppm PPCA or ATMP and the blank sample (SI = 0.31, C_{CaSO4}/solubility = 4.1, and C_{NaCl} = 0.25 M).

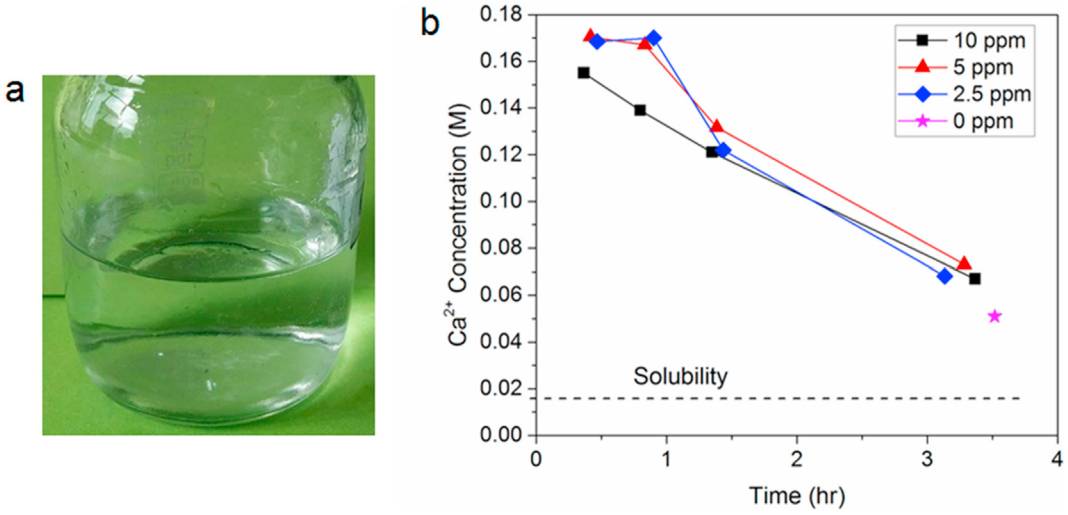

Figure 5. (a) Photograph of the supersaturated calcium sulfate sample with a saturation index of 0.31 containing 2.5 ppm PPCA two month after creating the supersaturation by mixing sulfate and calcium brines. (b) Calcium Concentration measured in different times after mixing the calcium and sulfate brines containing PPCA inhibitor at different concentrations (C_{CaSO4}/solubility = 10, C_{NaCl} = 0.5 M).

product. The band at 2948 cm^{-1} is due to CH_2 stretching vibrations in the alkane chain of the PPCA copolymer.

Figure 1b shows the ^{31}P NMR spectrum of the PPCA (Figure 1 c and d display magnified views of the same spectrum at different areas). According to previous works [28], the ^{31}P NMR of the phosphinic acid monomer exhibits one triplet, in which two symmetric peaks due to the coupling of P–H groups appear at the sides of the central peak due to the P atom. This characteristic triplet is absent in the spectrum of the PPCA product, which is a proof of successful formation of the product. The doublet peaks in the spectrum of the PPCA located at the chemical shift of 10–14 ppm correspond to the CH_2 groups directly bonded to the ^{31}P element, and the doublet located at 53–54 correspond to the next CH_2 group located two bonds away from the ^{31}P element. The peak at around 35 ppm can be assigned to the shielding effect of the P=O group [29]. Therefore, the IR and ^{31}P NMR spectra verify the formation of the PPCA compound.

In addition to structural characterizations, the molar mass of polymeric inhibitors is also an important parameter. Here, the determination of the molar mass was not possible using the gel permeation chromatography unfortunately, due to the highly acidic nature of the as-obtained PPCA sample [30]. However, based on previous reports the molar mass of the present PPCA copolymer should be in the range of 3500–4500 Da [31, 32].

3.2. Inhibition performance of PPCA

Before testing the performance of the as-synthesized PPCA inhibitor, the formation of the gypsum scale is verified by XRD. Figure 3 (a and b) shows the XRD pattern and the corresponding illustration of the crystal lattice for the gypsum precipitated from the uninhibited supersaturated solution at 25 °C. All the XRD peaks are attributed to the gypsum phase ($CaSO_4.2H_2O$, pdf number 033–0311) in accordance with previous XRD patterns for gypsum [33]. The very intense and narrow peaks indicate very large crystallite sizes.

Figure 4a shows the changes in the calcium ion concentration in 24 h for the samples containing 2.5 ppm PPCA, 2.5 ppm ATMP, and the blank sample. Figure 4b shows their associated curves based on Eq. (4), in which the slopes denote rate constants. The initial concentration of $Ca^{2+} = SO_4^{3-}$ = 75.5 mM is 4.1 times its solubility (18.3 mM) at 25 °C and the NaCl concentration is 0.25 M. In the blank sample after an induction time of about 1.5 h the first crystallites appear, and subsequently, the calcium concentration drops with a high rate to decrease the initial high thermodynamic driving force (-0.9 kJ/mol). Then, the curve approaches equilibrium very slowly, as the initial driving force has now decreased considerably. For the sample containing ATMP, a similar behavior is observed but with an increased induction time (5 h) and decreased reaction rate.

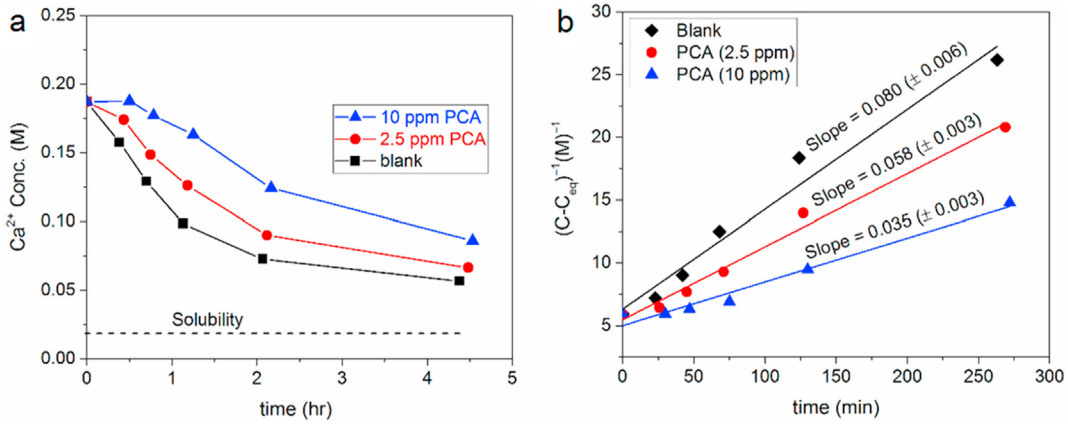

Figure 6. Calcium ion concentration at different times (a) and the corresponding rate constants (b) for samples containing 2.5 and 10 ppm PPCA and the blank sample (SI = 1.47, C_{CaSO4}/solubility = 10, and C_{NaCl} = 3 M).

Under the same condition (SI = 0.31, C_{CaSO4}/solubility = 4.1, and C_{NaCl} = 0.25 M), the sample containing PPCA (2.5 ppm) does not show any measurable drop in calcium ion concentration over 24 h. Interestingly, when this sample was sealed and kept under room temperature for two months, still no drop of concentration is measured and no crystallites were visually detected (Figure 5a).

In another experiment, when calcium sulfate concentration raised to 10 times its solubility (i.e., solubility = 0.0183 M, C_{CaSO4}/solubility = 10), but the concentration ratio of NaCl vs. $CaSO_4$ kept constant, the PPCA samples underwent a severe drop in the calcium concentration and performed only slightly better than the blank sample in the first 3.5 h (Figure 5b).

However, under the same condition with C_{CaSO4}/solubility = 10 when the added NaCl concentration increased from 0.5 M to 3 M the PPCA inhibitor showed improved performance. Figure 6a shows the C-t curves for the samples containing 10 ppm, 2.5 ppm, and 0 ppm (blank) PPCA at C_{CaSO4}/solubility of 10 during 4.5 h. Figure 6b displays the corresponding rate constants. The 10 ppm, 2.5 ppm, and 0 ppm PPCA samples show induction times of 1 h, 34 min, and 2 min, and the rate constants of 0.035, 0.058, and 0.080 L mol^{-1} min^{-1}, respectively. The higher dosages of PPCA had an inferior performance compared to the 10 ppm probably because at high dosages the highly acidic PPCA leads to a drop of pH to 4–5, while it is widely known that for polymeric inhibitors the optimum pH is 8–9.

Table 1 presents the performance of the PPCA (2.5 and 10 ppm) and its comparison with the ATMP and the blank sample. Here, in order to calculate the ion activities and the saturation indexes, the initial solution compositions were calculated using solution speciation in the PhreeqC program for the two different saturation indexes and the calculated data is outlined in Tables 2 and 3. Then, the initial Gibbs free energies were calculated based on Eq. (2). The inhibition efficiencies were calculated based on Eq. (5). For the saturation index of 0.31 the inhibition efficiencies are 100 % and 30.5 % for the 2.5 ppm PPCA and 2.5 ppm ATMP samples. For the saturation index of 1.47 the inhibition efficiencies are 24

Table 1. Thermodynamic and kinetic data for gypsum crystallization at 25 °C in the presence of NaCl supporting electrolyte at the starting pH of 8 (±0.5).

Sample (ppm)	NaCl Concentration	Saturation index	−ΔG (kJmol^{-1})	Induction time	Inhibition efficiency (%)	Rate constant (k, L mol^{-1} min^{-1})
PPCA (2.5)	0.25 M	0.31	0.9	>24 h	100%	~0*
ATMP (2.5)	0.25 M	0.31	0.9	5 h	30%	0.015
Blank	0.25 M	0.31	0.9	1.5 h	-	0.10
PPCA (2.5)	3 M	1.47	4.2	15 min	16%	0.058
PPCA (10)	3 M	1.47	4.2	1 h	24%	0.035
Blank	3 M	1.47	4.2	2 min	-	0.080

* Very small that it could not be measured by our method within the timescale of the experiment.

Table 2. Species distribution in the supersaturated solution (SI = 0.31) for gypsum formation obtained by PhreeqC program (error = 9%).

Species	Molality	Activity	Log Molality	Log Activity	Log Gamma	mole V cm^3/mol
OH^-	5.669e-06	2.694e-06	-5.246	-5.570	-0.323	4.00
H^+	4.474e-09	3.162e-09	-8.349	-8.500	-0.151	0.00
H_2O	5.551e+01	8.416e-01	1.744	-0.075	0.000	18.07
$CaHCO_3^+$	2.452e-05	1.503e-05	-4.611	-4.823	-0.213	10.07
$CaCO_3$	8.375e-06	2.935e-05	-5.077	-4.532	0.545	-14.60
HCO_3^-	4.888e-06	2.868e-06	-5.311	-5.542	-0.232	39.39
$NaHCO_3$	2.821e-06	9.884e-06	-5.550	-5.005	0.545	1.80
$NaCO_3^-$	1.621e-06	4.854e-06	-5.790	-5.314	0.476	26.74
CO_3^{2-}	3.589e-07	4.253e-08	-6.445	-7.371	-0.926	6.00
CO_2	6.914e-09	2.423e-08	-8.160	-7.616	0.545	34.43
$(CO_2)_2$	3.074e-18	1.077e-17	-17.512	-16.968	0.545	68.87
Ca^{2+}	5.014e-01	4.108e-01	-0.300	-0.386	-0.087	-14.49
$CaSO_4$	5.561e-02	1.948e-01	-1.255	-0.710	0.545	7.50
$CaHCO_3^+$	2.452e-05	1.503e-05	-4.611	-4.823	-0.213	10.07
$CaCO_3$	8.375e-06	2.935e-05	-5.077	-4.532	0.545	-14.60
$CaOH^+$	6.061e-06	1.814e-05	-5.217	-4.741	0.476	(0)
$CaHSO_4^+$	1.353e-09	4.050e-09	-8.869	-8.393	0.476	(0)
Cl^-	4.317e+00	2.589e+00	0.635	0.413	-0.222	20.01
Na^+	4.258e+00	6.129e+00	0.629	0.787	0.158	1.13
$NaSO_4^-$	1.397e-01	8.194e-02	-0.855	-1.086	-0.232	36.70
$NaHCO_3$	2.821e-06	9.884e-06	-5.550	-5.005	0.545	1.80
$NaCO_3^-$	1.621e-06	4.854e-06	-5.790	-5.314	0.476	26.74
NaOH	4.712e-16	1.651e-15	-15.327	-14.782	0.545	(0)
$NaSO_4^-$	1.397e-01	8.194e-02	-0.855	-1.086	-0.232	36.70
$CaSO_4$	5.561e-02	1.948e-01	-1.255	-0.710	0.545	7.50
SO_4^{2-}	4.256e-02	2.668e-03	-1.371	-2.574	-1.203	23.20
$CaHSO_4^+$	1.353e-09	4.050e-09	-8.869	-8.393	0.476	(0)
HSO_4^-	2.740e-10	8.201e-10	-9.562	-9.086	0.476	41.98

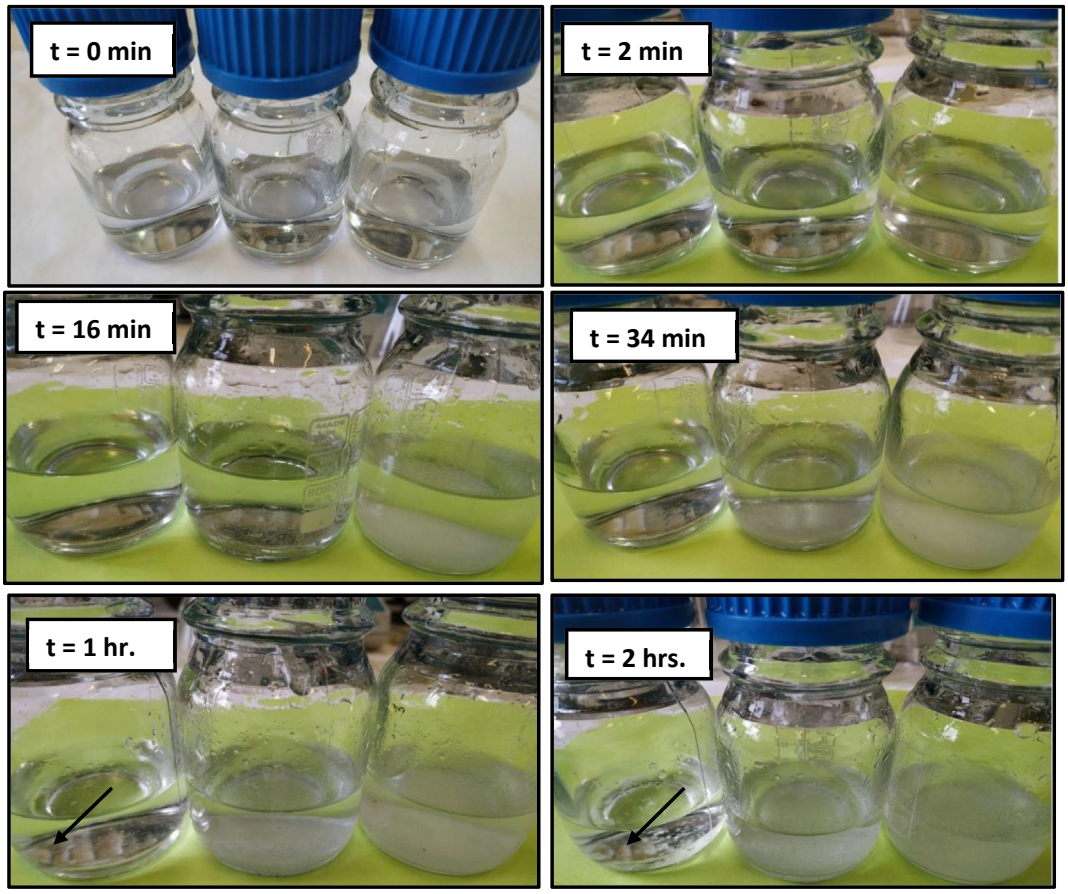

Figure 7. Photographs of the supersaturated samples containing 10 ppm PPCA (left bottle), 2.5 ppm PPCA (middle bottle) and 0 ppm PPCA (right bottle) with SI = 1.47 and the added NaCl concentration of 3 M at different times. (the arrows indicate gypsum).

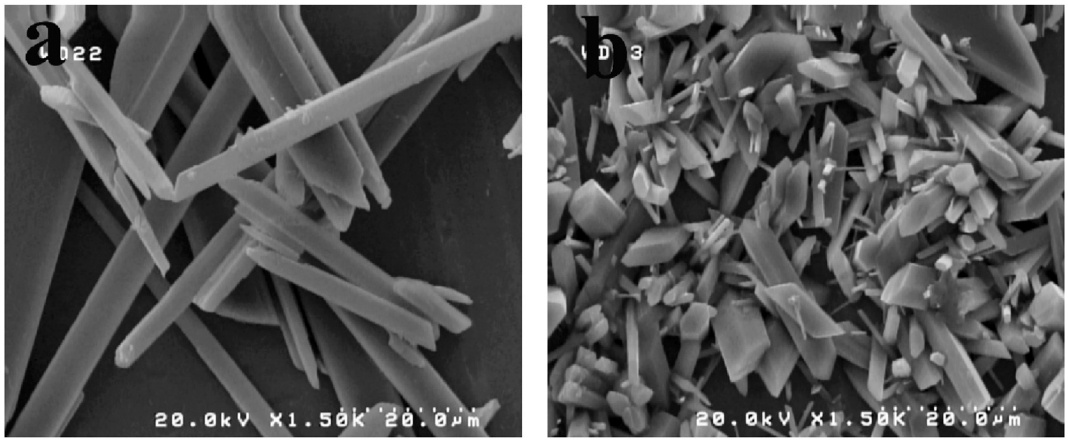

Figure 8. FESEM images of the gypsum precipitated from a) supersaturated blank sample after 1 day and (b) the sample containing 2.5 ppm PPCA after two months. (SI = 0.31 and C_{NaCl} = 0.25 M).

% and 16 % for the 10 ppm and 2.5 ppm PPCA samples. The photographs in Figure 7 exhibit the evolution of the gypsum crystallites for these samples over the time of 4.5 h at the saturation index of 1.47.

In order to investigate the effect of the PPCA inhibitor on the crystal morphology of the formed gypsum, FESEM images were also recorded. Figure 8 (a and b) shows the FESEM images of the gypsum precipitated under same condition from the blank sample and the sample containing 2.5 ppm PPCA at an SI of 0.31 (C_{CaSO4}/solubility = 4.1), respectively. For the blank sample, the gypsum crystals have grown in their regular fiber-shaped morphology with diameter of about 5 μm, but for the inhibited sample the gypsum crystals have grown quite irregularly with smaller particle dimension of about 2 μm.

4. Discussion

The mechanism of scale inhibition by chemical inhibitors is an open subject that is widely debated [34]. Generally, induction times are associated with nucleation kinetics, and the calculated rate constants are associated with growth rates. Since, here the PPCA has caused an increase in the induction times and a reduction in the rate constants, it is

Table 3. Species distribution in the supersaturated solution (SI = 1.47) for gypsum formation obtained by PhreeqC (error = 7%).

Species	Molality	Activity	Log Molality	Log Activity	Log Gamma	mole V cm^3/mol
OH^-	5.148e-06	3.146e-06	-5.288	-5.502	-0.214	-2.66
H^+	4.185e-09	3.162e-09	-8.378	-8.500	-0.122	0.00
H_2O	5.551e+01	9.831e-01	1.744	-0.007	0.000	18.07
HCO_3^-	1.816e-05	1.229e-05	-4.741	-4.910	-0.169	26.92
$CaCO_3$	6.269e-06	7.291e-06	-5.203	-5.137	0.066	-14.60
$CaHCO_3^+$	5.385e-06	3.734e-06	-5.269	-5.428	-0.159	9.96
$NaHCO_3$	1.747e-06	2.032e-06	-5.758	-5.692	0.066	1.80
$NaCO_3^-$	1.340e-06	9.979e-07	-5.873	-6.001	-0.128	2.78
CO_3^{2-}	8.685e-07	1.823e-07	-6.061	-6.739	-0.678	-2.03
CO_2	7.645e-08	8.891e-08	-7.117	-7.051	0.066	34.43
$(CO_2)_2$	1.248e-16	1.451e-16	-15.904	-15.838	0.066	68.87
Ca^{2+}	9.495e-02	2.381e-02	-1.023	-1.623	-0.601	-16.71
$CaSO_4$	8.362e-03	9.725e-03	-2.078	-2.012	0.066	7.50
$CaCO_3$	6.269e-06	7.291e-06	-5.203	-5.137	0.066	-14.60
$CaHCO_3^+$	5.385e-06	3.734e-06	-5.269	-5.428	-0.159	9.96
CaOH+	1.649e-06	1.228e-06	-5.783	-5.911	-0.128	(0)
$CaHSO_4^+$	2.714e-10	2.021e-10	-9.566	-9.694	-0.128	(0)
Cl^-	4.663e-01	2.949e-01	-0.331	-0.530	-0.199	18.78
Na^+	4.098e-01	2.940e-01	-0.387	-0.532	-0.144	-0.52
$NaSO_4^-$	5.000e-03	3.384e-03	-2.301	-2.471	-0.169	21.09
$NaHCO_3$	1.747e-06	2.032e-06	-5.758	-5.692	0.066	1.80
$NaCO_3^-$	1.340e-06	9.979e-07	-5.873	-6.001	-0.128	2.78
NaOH	7.954e-17	9.249e-17	-16.099	-16.034	0.066	(0)
SO_4^{2-}	1.248e-02	2.297e-03	-1.904	-2.639	-0.735	17.45
$CaSO_4$	8.362e-03	9.725e-03	-2.078	-2.012	0.066	7.50
$NaSO_4^-$	5.000e-03	3.384e-03	-2.301	-2.471	-0.169	21.09
HSO_4^-	9.481e-10	7.063e-10	-9.023	-9.151	-0.128	40.95
$CaHSO_4^+$	2.714e-10	2.021e-10	-9.566	-9.694	-0.128	(0)

implied that it acts based on inhibiting both the nucleation and growth processes, as it is expected for polymer-based inhibitors. On a molecular level, it has been reported that polymer inhibitors are principally nucleation inhibitors through their reaction with newly-formed ionic clusters and causing them re-dissolve [12].

Besides, the experiments at different sodium chloride concentrations here show the obvious impact of this salt on the scaling tendency and the inhibition properties of the PPCA copolymer. This effect could be through changing the ionic strength of the oilfield produced water and the properties of the inhibitor. With increasing the concentration of NaCl from 0.25 M to 3 M and increasing the concentration of calcium sulfate ions (1:1) from 0.075 M to 0.183 M, the calculated ionic strength increases from 0.65 mol/kgw to 5.44 mol/kgw (in molality unit). However, interestingly, the calculated activity coefficient (and the activity) increase from 0.25 to 0.8, leading to an increase in the saturation index from 0.31 to 1.47. Therefore, the reason behind such a loss of performance for the PPCA inhibitor at the high calcium sulfate concentration of 0.183 M is the curving up of the activity coefficient-ionic strength which leads to an extremely high saturation index and thermodynamic driving force (Tables 1,2, and 3). Nevertheless, most studies are focused on the bulk solution with conventional concentrations, while for high saturation indexes scaling tendency would be highly enhanced as shown here [35].

5. Conclusion

Sulfate-based scales are a bottleneck of many industrial water equipment including the Siri Island oil production fields in the south of Iran. Here, the synthesis and performance analyses of a phosphino-polycarboxylic acid (PPCA) copolymer were presented as an efficient scale inhibitor that is more environmentally benign compared to (poly) phosphonates for application under normal conditions. The analyses showed that the as-synthesized PPCA without any pH and temperature regulations can completely prevent gypsum scaling at an SI of 0.31, and in conjunction with the NaCl supporting electrolyte it still shows an inhibition efficiency of 24% at an extremely high SI of 1.47.

Declarations

Author contribution statement

K. Malaie and O. Shojaei: Conceived and designed the experiments; Performed the experiments; Analyzed and interpreted the data; Wrote the paper.

S. Iranpour and Z. Taherkhani: Contributed reagents, materials, analysis tools and data.

Funding statement

This work was supported by the Chemical Process Design Research Group for the ACECR at the University of Tehran.

Data availability statement

Data included in article/supplementary material/referenced in article.

Declaration of interests statement

The authors declare no conflict of interest.

Additional information

No additional information is available for this paper.

Acknowledgements

The authors would like to thank Dr. Aseyeh Ghaedi for her assistance in analyzing the ^{31}PNMR spectra and also Dr. Zahra Heydari for her assistance in recording the XRD spectra.

References

[1] M. El-Said, M. Ramzi, T. Abdel-Moghny, Analysis of oilfield waters by ion chromatography to determine the composition of scale deposition, Desalination 249 (2009) 748–756.
[2] A. Zeino, M. Albakri, M. Khaled, M. Zarzour, Comparative study of the synergistic effect of ATMP and DTPMPA on CaSO4 scale inhibition and evaluation of induction time effect, J. Water Process Eng. 21 (2018) 1–8.
[3] X. Liu, T. Chen, P. Chen, H. Montgomerie, T. Hagen, B. Wang, X. Yang, Understanding the co-deposition of calcium sulphate and barium sulphate and developing environmental acceptable scale inhibitors applied in HTHP wells, Soc. Pet. Eng. - SPE Int. Conf. Exhib. Oilf. Scale 2012 (2012) 607–616.
[4] Y.N. Wang, E. Järvelä, J. Wei, M. Zhang, H. Kyllönen, R. Wang, C.Y. Tang, Gypsum scaling and membrane integrity of osmotically driven membranes: the effect of membrane materials and operating conditions, Desalination 377 (2016) 1–10.
[5] D.E. Abd-El-Khalek, B.A. Abd-El-Nabey, M.A. Abdel-Kawi, S. Ebrahim, S.R. Ramadan, The inhibition of crystal growth of gypsum and barite scales in industrial water systems using green antiscalant, Water Sci. Technol. Water Supply 19 (2019) 2140–2146.
[6] Y. Chen, Y. Zhou, Q. Yao, Y. Bu, H. Wang, W. Wu, W. Sun, Evaluation of a low-phosphorus terpolymer as calcium scales inhibitor in cooling water, Desalin. Water Treat. 55 (2015) 945–955.
[7] W. Wang, A.T. Kan, M.B. Tomson, B. Chemistry, A Novel and Comprehensive Study of Polymeric and Traditional Phosphonate Inhibitors for High-Temperature Scale Control, 2012, pp. 30–31.
[8] B. Senthilmurugan, B. Ghosh, S.S. Kundu, M. Haroun, B. Kameshwari, Maleic acid based scale inhibitors for calcium sulfate scale inhibition in high temperature application, J. Petrol. Sci. Eng. 75 (2010) 189–195.
[9] Y.A. Maher, M.E.A. Ali, H.E. Salama, M.W. Sabaa, Preparation, characterization and evaluation of chitosan biguanidine hydrochloride as a novel antiscalant during membrane desalination process, Arab. J. Chem. 13 (2020) 2964–2981.
[10] Z. Amjad, Calcium sulfate dihydrate (gypsum) scale formation on heat exchanger surfaces: the influence of scale inhibitors, J. Colloid Interface Sci. 123 (1988) 523–536.
[11] A. Hina, G.H. Nancollas, Precipitation and dissolution of alkaline earth sulfates: kinetics and surface energy, Rev. Mineral. Geochem. 40 (2000) 277–301.
[12] S. Carvalho, L. Palermo, L. Boak, K. Sorbie, E.F. Lucas, Influence of terpolymer based on amide, carboxylic, and sulfonic groups on the barium sulfate inhibition, Energy Fuel. 31 (2017) 10648–10654.
[13] K.K. Sand, D.J. Tobler, S. Dobberschütz, K.K. Larsen, E. Makovicky, M.P. Andersson, M. Wolthers, S.L.S. Stipp, Calcite growth kinetics: dependence on saturation index, Ca2+:CO32- activity ratio, and surface atomic structure, Cryst. Growth Des. 16 (2016) 3602–3612.
[14] H. Luo, D. Chen, X. Yang, X. Zhao, H. Feng, M. Li, J. Wang, Synthesis and performance of a polymeric scale inhibitor for oilfield application, J. Pet. Explor. Prod. Technol. 5 (2015) 177–187.
[15] M. Andrei, A. Malandrino, Comparative coreflood studies for precipitation and adsorption squeeze with PPCA as the scales inhibitor, Petrol. Sci. Technol. 21 (2003) 1295–1315.
[16] N.M. Farooqui, K.S. Sorbie, The use of PPCA in scale-inhibitor precipitation squeezes: solubility, inhibition efficiency, and molecular-weight effects, SPE Prod. Oper. 31 (2016) 258–269.
[17] M.C. Van Der Leeden, G.M. Van Rosmalen, Effect of the molecular weight of polyphosphinoacrylates on their performance in BaSO4 growth retardation, J. Cryst. Growth 100 (1990) 109–116.
[18] T. Chen, A. Neville, K. Sorbie, Z. Zhong, In-situ monitoring the inhibiting effect of polyphosphinocarboxylic acid on CaCO3 scale formation by synchrotron X-ray diffraction, Chem. Eng. Sci. 64 (2009) 912–918.
[19] M.A. Smith, M. J, P. Miles, N. Richardson, Finan, Inhibiting Scale Formation in Aqueous Systems, U.K. GB 1458235, 1976.
[20] A.B. BinMerdhah, Inhibition of barium sulfate scale at high-barium formation water, J. Petrol. Sci. Eng. 90–91 (2012) 124–130.
[21] N.M. Farooqui, A. Grice, K.S. Sorbie, D. Haddleton, Polyphosphino carboxylic acid (PPCA) scale inhibitor for application in precipitation squeeze treatments: the effect of molecular weight distribution, NACE - Int. Corros. Conf. Ser. (2014) 1–16.
[22] P. Zhang, D. Shen, A.T. Kan, M.B. Tomson, Phosphino-polycarboxylic acid modified inhibitor nanomaterial for oilfield scale control: transport and inhibitor return in formation media, RSC Adv. 6 (2016) 59195–59205.
[23] H. Watson, A.J. Cockbain, J. Spencer, A. Race, M. Volpato, P. Loadman, G. Toogood, M.A. Hull, Adsorption of polyphosphinocarboxylic acid (PPCA) scale inhibitor on carbon nanotubes (CNTs): a prospective method for enhanced oilfield scale prevention, Prostaglandins Leukot. Essent. Fatty Acids 115 (2016) 60–66.
[24] L.L. Zhao, Y. Liu, J. Chen, Synthesis of phosphoryl carboxylic acid terpolymer as scale inhibitors, J. Chem. Ind. Eng. 35 (2014) 36–38. http://en.cnki.com.cn/Article_en/CJFDTOTAL-HXGJ201405014.htm.
[25] Mingzhu Xia, Synthesis and Performance of Phosphono Carboxylic Acid, Nanjing University of Science and Technology, Nanjing, 2006.
[26] G.H. Nancollas, A.E. Eralp, J.S. Gill, Calcium sulfate scale formation: a kinetic approach, Soc. Pet. Eng. AIME J. 18 (1978) 133–138.
[27] R.D. Ramsier, P.N. Henriksen, A.N. Gent, Adsorption of phosphorus acids on alumina, Surf. Sci. 203 (1988) 72–88.
[28] N.S. Golubev, R.E. Asfin, S.N. Smirnov, P.M. Tolstoi, Study of hydrogen bonds of hypophosphorous acid by 1H, 2H, 31P, and 15N NMR spectroscopy under slow exchange conditions, Russ. J. Gen. Chem. 76 (2006) 915–924.
[29] V. Iaroshenko, Modern aspects of 31 P NMR spectroscopy, Organophos. Chem. (2019) 457–498.
[30] M.R. Dubay, The Molecular Weight Effects of Poly(acrylic Acid) on Calcium Carbonate Inhibition in the Kraft Pulping Process, 2011.
[31] J.A. Xiao, Acid - Base and Metal Complexation Chemistry of Phosphino-Polycarboxylic Acid under High Ionic Strength and High Temperature, 2001, pp. 4661–4667.
[32] P.E. Hruskoci, United States Patent (19), 2000.
[33] N. Prieto-Taboada, A. Larrañaga, O. Gómez-Laserna, I. Martínez-Arkarazo, M.A. Olazabal, J.M. Madariaga, The relevance of the combination of XRD and Raman spectroscopy for the characterization of the CaSO4-H2O system compounds, Microchem. J. 122 (2015) 102–109.
[34] M. Oshchepkov, S. Kamagurov, S. Tkachenko, A. Ryabova, K. Popov, Insight into the mechanisms of scale inhibition: a case study of a task-specific fluorescent-tagged scale inhibitor location on gypsum crystals, Chem. Nano. Mat. 5 (2019) 586–592.
[35] G. Suo, L. Xie, S. Xu, L. Feng, T. Dong, X. Shao, Study on inhibitors' performance under the condition of high concentration ratio in MED system, Desalination 437 (2018) 100–107.